

# Optical properties of silicon nanoclusters fabricated by ion implantation

Tsutomu Shimizu-Iwayama<sup>a)</sup> and Norihiro Kurumado

*Department of Materials Science, Aichi University of Education, Igaya-cho, Kariya-shi, Aichi 448-8542, Japan*

David E. Hole and Peter D. Townsend

*School of Engineering, University of Sussex, Falmer, Brighton BN1 9QH, United Kingdom*

(Received 23 January 1998; accepted for publication 27 February 1998)

A method for the fabrication of luminescent Si nanoclusters in an amorphous SiO<sub>2</sub> matrix by ion implantation is reported. We have measured the dose (concentration of excess Si atoms) and annealing time dependence of the photoluminescence of Si nanoclusters in SiO<sub>2</sub> layers at room temperature. The samples were fabricated by ion implantation and subsequent annealing. After annealing, a photoluminescence band below 1.7 eV has been observed. The peak energy of the photoluminescence is found to be almost independent of annealing time, while the intensity of the luminescence increases as the annealing time increases. Moreover, we found that the peak energy of the luminescence is strongly affected by the dose of implanted Si ions, especially in the high-dose range. We also show direct evidence of widening of the band-gap energy of Si particles of a few nanometers in size by employing photoacoustic spectroscopy. These results indicate that the photons are absorbed by Si nanoclusters, for which the band-gap energy is modified by the quantum confinement effects, and the emission is not simply due to direct electron-hole recombination inside Si nanoclusters, but is related to defects probably at the interface between the Si nanoclusters and SiO<sub>2</sub>, for which the energy state is affected by cluster-cluster interactions. © 1998 American Institute of Physics. [S0021-8979(98)03411-2]

## INTRODUCTION

In recent years, there has been considerable interest in semiconductor nanostructures, especially porous Si (Refs. 1 and 2) and Si ultrafine particles,<sup>3-7</sup> which are fabricated by several methods and exhibit strong visible luminescence even at room temperature. Nanometer-sized particles show unique electrical and optical properties, which are not observed in bulk materials. Although there has been a considerable amount of investigation, the mechanism for luminescence from these Si nanostructures is still unclear.

One approach to produce nanoclusters, compatible with conventional microelectronic technology, may be by ion implantation. The ion-implantation technique has the advantage that given numbers of ions can be placed in a controlled depth distribution by changing the ion doses and the acceleration energies.<sup>8,9</sup> Ion-beam synthesis of Si nanoclusters is a potential candidate for the method of manufacturing pure Si nanoclusters, not only for basic research, but also for application for monolithically integrated Si-based optoelectronic devices.

The present authors have carried out a series of studies on the structural properties and the luminescence behaviors of high-energy (1 MeV) and relatively low-dose Si<sup>+</sup>-implanted silica glasses<sup>10-12</sup> and thermal oxide films grown on Si wafers.<sup>13-15</sup> We have shown that these specimens exhibit two luminescence bands in the visible range. One peaked around 2.0 eV, which is observed in as-implanted specimens and those annealed at about 600 °C,

which can be attributed to excess Si defects. The other peaked around 1.7 eV, which is observed only after annealing specimens with higher temperature.

After our first reports,<sup>10</sup> a rush of papers<sup>16-20</sup> concerning to the 1.7 eV luminescence appeared employing the technique of Si ion implantation into SiO<sub>2</sub> and subsequent high-temperature annealing. More recently, electroluminescence from Si ion-implanted thermal oxide films has also been reported.<sup>21</sup> Although the 1.7 eV luminescence is evidently related to Si nanoclusters formed by decomposition of the SiO<sub>x</sub> phase with high-temperature annealing, the detailed mechanism of the luminescence is not yet clear. The purpose of this paper is to report the wide range of dose (concentration of implanted excess Si atoms) and annealing time effects on the luminescence from the ion-implanted layer, and the optical absorption of Si nanoparticles produced by gas evaporation techniques, and to discuss the detailed mechanism for the 1.7 eV luminescence of the Si<sup>+</sup>-implanted layer.

## EXPERIMENT

The samples were prepared by implanting Si ions into an oxidized Sb-doped Si epitaxial layer (10 Ω cm, 10 μm) grown on p<sup>+</sup>-type Si wafers with a resistance of around 0.01 Ω cm (oxide thickness of 300 and 600 nm). Ion implants were made with a Whickham ion implanter over the energy range from 25 to 200 keV with a beam current of 570 μA (current density of about 28.5 μA/cm<sup>2</sup>). The results for two different types of samples are presented here. One type of sample (type A) was prepared by the implantation of Si ions into an oxide film of 600 nm thickness at an energy of 180

<sup>a)</sup>Corresponding author. Electronic mail: tiwayama@aecc.aichi-edu.ac.jp

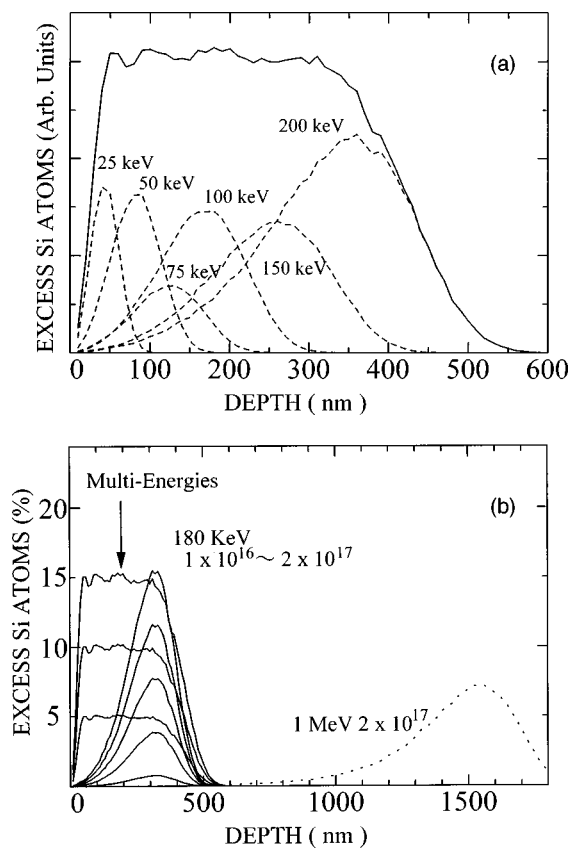


FIG. 1. Estimated depth profiles obtained by using SRIM program. (a) Uniform profiles (sample B), (b) All of samples used in the experiments. A depth profile of 1 MeV Si, used in our previous work, is also shown in the figure.

keV with doses from  $1 \times 10^{16}$  to  $2 \times 10^{17}$  ions/cm<sup>2</sup>. The other type of sample (type B) was prepared by implanting Si ions at six energies between 25 and 200 keV with varying doses to produce uniform excess Si concentrations of 5%, 10%, and 15% in an oxide film of 300 nm thickness on Si wafers. The expected depth profiles of implanted Si atoms in thermal oxide films on Si wafers were estimated using SRIM (the stopping and range of ions in matter),<sup>22</sup> as shown in Figs. 1(a) and 1(b). All implantations were performed at room temperature. The samples were then annealed at 1050 °C in a N<sub>2</sub> atmosphere for several hours to induce precipitation and the formation of Si nanoclusters.

Si ultrafine particles (UFP) were also fabricated by gas evaporation techniques.<sup>6,23</sup> The process chamber was filled with He gas to a pressure of 3 Torr and Si was evaporated. Si UFP were deposited onto high-purity fused silica substrates, which were used as specimens. The sizes of the Si UFP were confirmed by scanning electron microscope measurements and found to be distributed around a few nanometers. Heat treatment of the specimens was carried out in an Ar or O<sub>2</sub> gas ambient using an infrared lamp annealing system.

Photoluminescence spectra were measured at room temperature in a conventional way. An Ar-ion laser (2.41 or 2.54 eV) was used as an excitation source and the luminescence was detected by a cooled photomultiplier tube, employing the photon-counting technique. Photoacoustic spectra were obtained by the use of a standard apparatus<sup>24,25</sup> fitted with a

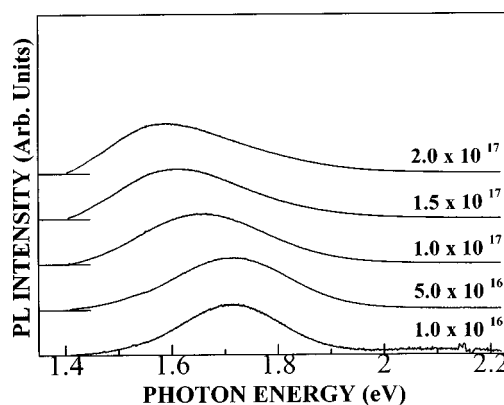


FIG. 2. Photoluminescence spectra of 180 keV Si<sup>+</sup>-implanted 600 nm thermal oxide films at doses of  $1 \times 10^{16}$ ,  $5 \times 10^{16}$ ,  $1 \times 10^{17}$ ,  $1.5 \times 10^{17}$ , and  $2 \times 10^{17}$  ions/cm<sup>2</sup> (from bottom to top) and excited with a 2.54 eV laser, after annealing at 1050 °C for 4 h. The zero lines of some curves are shifted vertically.

500 W Xe lamp. The monochromatized light beam from the lamp was focused onto a light chopper operating at 20 Hz and focused again onto the samples, which were placed in a closed photoacoustic cell. The signal detected by a high-sensitivity microphone was preamplified and routed to a lock-in amplifier.

## EXPERIMENT RESULTS

The photoluminescence spectra of type A samples after annealing at 1050 °C for 4 h are shown in Fig. 2. A laser line of 2.54 eV was used as an excitation source to obtain all of the luminescence spectra shown hereafter, except for a part of the spectra shown in Fig. 5. The intensities of the luminescence are normalized at the peak height, and the zero lines of some curves are shifted vertically to compare the peak energies of the luminescence. It is clear from the figures that the peak energies of the luminescence spectra are strongly affected by the doses of implanted Si ions in the high-dose range. The peak energies are close to 1.7 eV in samples with lower doses (below a dose of  $5 \times 10^{16}$  ions/cm<sup>2</sup>), but are shifted to lower energies with increasing dose of implanted Si ions. It is noted that the peak energy of the luminescence spectra after annealing for these samples is also found to be independent of the annealing time. However, the intensity of the luminescence is affected by both the annealing time and the dose of implanted Si ions. The luminescence intensity grows and then saturates, as the annealing time increases.

For the purpose of discussing the detail correlations between the concentrations of implanted excess Si atoms and the luminescence, we also obtained the photoluminescence spectra of a Si<sup>+</sup>-implanted layer with uniform excess Si concentrations. The photoluminescence spectra of type B samples after annealing at 1050 °C for 8 h are shown in Fig. 3. It is also clear from the figures that the peak energies and the intensities of the luminescence are strongly affected by the concentrations of implanted excess Si atoms. The peak is shifted to lower energies with increasing concentrations of excess Si atoms, similar to that observed in type A samples.

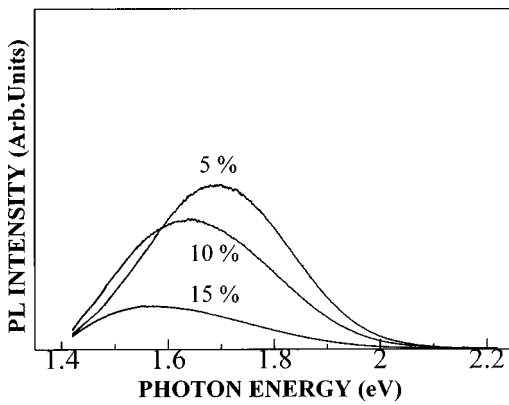


FIG. 3. Photoluminescence spectra of type B samples with concentrations of 5%, 10%, and 15% implanted excess Si atoms and excited with a 2.54 eV laser, after annealing at 1050 °C for 8 h.

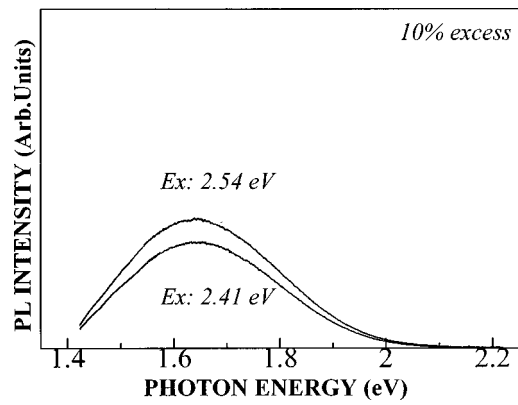


FIG. 5. Photoluminescence spectra of type B samples with 10% excess Si and excited with 2.41 and 2.54 eV laser, after annealing at 1050 °C for 8 h.

The time evolution of the photoluminescence spectra of type B samples with annealing at 1050 °C for several hours are shown in Figs. 4(a) and 4(b). It is clear from the figures that the luminescence intensity grows as the annealing time increases and the peak energies of the luminescence spectra are independent of the annealing time. It is noted that the shape of the luminescence spectra after annealing is also found to be independent of the annealing time in all of the samples. We obtained the luminescence spectra excited with laser lines at both 2.41 and 2.54 eV in all samples. One of the results is shown in Fig. 5. It is clear that the luminescence

spectra are independent of the excitation energies. The peak energies of the luminescence spectra are independent of excitation energies. The difference of the excitation energy of 2.41 eV from that of 2.54 eV arises only in the difference in the decrease of luminescence intensity. It is noted that similar experimental results were obtained in all of the samples.

The photoacoustic spectrum of an as-prepared nanometer-sized Si UFP sample is shown in Fig. 6(A). The spectrum of bulk Si is also shown in the figure. The band-gap energy of Si UFP increases when compared to that of

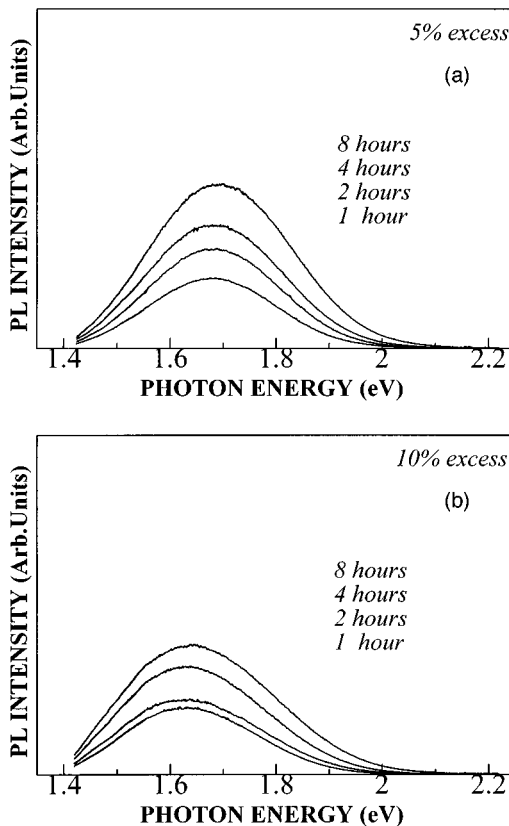


FIG. 4. Photoluminescence spectra of type B samples. (a) 5% and (b) 10% excess implanted Si atoms and excited with 2.54 eV laser, after annealing at 1050 °C for 1, 2, 4, and 8 h (from bottom to top).

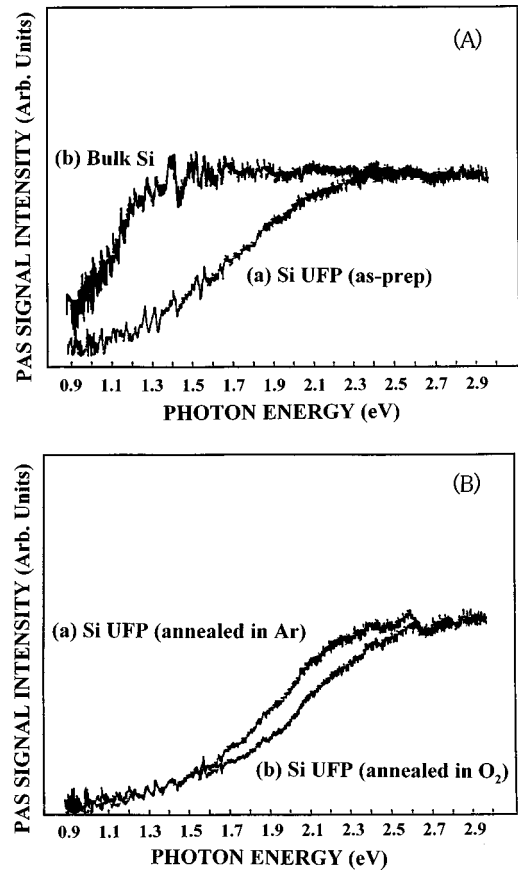


FIG. 6. (A) Photoacoustic spectra of (a) gas evaporated Si and (b) bulk Si and (B) photoacoustic spectra of gas evaporated Si after annealing at 500 °C for 1 h in (a) Ar and (b) O<sub>2</sub> atmosphere.

bulk Si. Additionally, we annealed the specimens at 500 °C for 1 h in Ar and O<sub>2</sub> atmospheres, and measured photoacoustic spectra. The results are shown in Fig. 6(B). It is clear that the band-gap energies increase with annealing in both specimens, although the increase is more significant in the specimen annealed in O<sub>2</sub> atmosphere. It is noted that the luminescence around 1.7 eV, similar to that observed in heat treated Si<sup>+</sup>-implanted samples, is observed only for the specimen annealed in an O<sub>2</sub> atmosphere.

## DISCUSSION

In this section, we discuss the correlation between the microstructure of the Si<sup>+</sup>-implanted layer and the luminescence band around 1.7 eV observed after annealing above 1050 °C. Initially, however, we would like to review our previous experimental results of cross-section high-resolution transmission electron microscopy.<sup>15</sup> We reported that no trace of the formation of crystalline Si is evident before heat treatment, however, the micrograph after heat treatment at high temperature indicates Si nanoclusters in an amorphous SiO<sub>2</sub> matrix for samples implanted with 1 MeV Si ions to a dose of  $2 \times 10^{17}$  ions/cm<sup>2</sup> around the depth of the projected range of the implanted Si [around the depth of 1.5 μm, as shown in Fig. 1(b)]. Moreover, we observed growth in the size of Si clusters after increasing the annealing time.

According to the results of photoacoustic spectroscopy, the band-gap energy of Si in the range of a few nanometers evidently increases compared to that of bulk Si, as expected by quantum confinement effects.<sup>26</sup> The change of the spectra seen with annealing in an Ar ambient can probably be explained by the crystallization of Si UFP. However, in the case of annealing in an O<sub>2</sub> ambient, Si UFP are oxidized and the mean-core size of Si UFP becomes smaller than those annealed in Ar ambient. There is no clear evidence for the correlation between the size and the band-gap energy, however, we can see here that the band-gap energy of Si particles of a few nanometers in size is quite different from that of bulk crystalline Si.

From the experimental results obtained from photoacoustic spectroscopy and the dose dependence of the photoluminescence of Si nanoclusters alone, it seems that the origin of the luminescence is due to the quantum confinement effects and simply related to direct electron–hole recombination inside Si nanoclusters. But we have to discuss the mechanism of luminescence carefully. An important point to note is that the luminescence intensity grows during annealing, without changing the peak energy of the luminescence, in all samples investigated. Since the size of the Si nanoclusters evidently grows as the annealing time increases, the absence of the dependence of the peak energy of the luminescence spectra on the annealing time excludes the possibility that the luminescence is simply due to the direct recombination between electrons and holes confined in the inside of Si nanoclusters.

The results in the present experiments seem to be consistent with the presumption that the absorption of photons leads to the generation of electron–hole pairs, which are con-

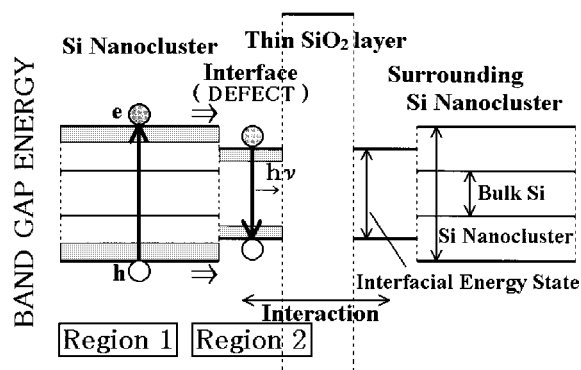


FIG. 7. Schematic illustration of a reactive nanocluster model of photoluminescence in which the nanoclusters react via a thin oxide interface.

finer in the Si nanoclusters, while the emission of photons originates at the interface between Si nanoclusters and the SiO<sub>2</sub> matrix, as previously proposed by Kanemitsu *et al.*<sup>27</sup> For a smaller average size, adsorbed photons with higher energies can contribute to the luminescence. Based on this model, we can explain that the peak energy of the luminescence after annealing is independent of the annealing time, and is also independent of the excitation energies. However, with this so-called three-region model, we cannot explain the dose-dependent shift of the photoluminescence of Si nanoclusters.

Here, we propose a model named the “reactive nanocluster model,” as shown in Fig. 7. In this model, we will also take into account factors other than the size of Si nanoclusters. We consider that the band-gap widening due to the quantum confinement effect plays an essential role in the photoabsorption process (region 1) and the interface energy state between the Si nanoclusters and thin SiO<sub>2</sub> layer, for which the energy state is affected by cluster–cluster interactions via a thin oxide interface, plays an essential role in the luminescence process (region 2). In most reports concerning porous Si and other Si nanostructures, only the correlation between the size of the Si clusters and the peak energy of the luminescence has been discussed. Here, we would like to stress the importance of the local concentrations of Si nanoclusters. If the Si nanoclusters have been concentrated, interactions between Si nanoclusters via a thin oxide and a decrease in the interfacial energy state should be expected. With an increase in the implanted Si dose, of course, the local concentration of Si atoms increases, and this increase in the local concentration of Si seems to contribute to both the size and the number of Si nanoclusters. However, once the nucleation of clusters occurs by decomposition of SiO<sub>x</sub>, a point would be reached where Si clusters formed would not migrate in a SiO<sub>2</sub> matrix and the number of clusters is, thus, not so changed with prolonged annealing.

Based on these assumptions, we can explain our present experimental results as follows. Because the number of the Si nanoclusters is almost fixed with prolonged annealing and only growth in the size of clusters occurs, the change in the distance between mutual clusters is negligible, even if the size increases. In contrast to this, with an increase in the dose of implanted Si ions, the number of Si clusters increases.

Then, the mutual distance between nanoclusters changes, and cluster-cluster interactions via a thin oxide can be expected. Below the dose of  $5 \times 10^{16}$  ions/cm<sup>2</sup> with an energy of 180 keV, the peak energy is almost fixed around 1.7 eV. This energy seems to be the interfacial energy state between Si nanoclusters and the SiO<sub>2</sub> matrix without interactions. More recently, tunable<sup>28</sup> and blue<sup>29</sup> luminescence has been reported in ion-implanted specimens annealed in a reactive gas atmosphere. These results also suggest the importance of the interfacial regions.

In conclusion, we measured dose and annealing time dependence of the photoluminescence of Si nanoclusters in SiO<sub>2</sub> layers, fabricated by ion implantation and subsequent annealing, at room temperature. We found that the peak energy of the photoluminescence is independent of annealing time and excitation energy, while the intensity of the luminescence increases as the annealing time and excitation energy increases. Moreover, we found that the peak energy of the luminescence is strongly affected by the dose of implanted Si ions, especially in the high-dose range. These experimental results are in good qualitative agreement with a reactive nanocluster model. We also found that the density of the Si nanoclusters was an important factor to discuss the luminescence from Si nanostructures. This method of fabricating Si nanoclusters by ion implantation and subsequent annealing is an important technique to discriminate between the contributions of the size and the concentration of Si nanoclusters to the luminescence. Further studies on the direct observation of the size and the concentration of Si nanoclusters in Si ion-implanted SiO<sub>2</sub> layers are now in progress.

## ACKNOWLEDGMENTS

The authors would like to express their gratitude to Makoto Takiyama, Nippon Steel Corporation, for supplying Si wafers with thermal oxide films and to Dr. J. F. Ziegler, IBM-Research for providing the program disk of SRIM. This work has been partly supported by the Nippon Sheet Glass Foundation, the Foundation for Materials Science and Engineering, the Iketani Science and Technology Foundation, and the Japan Securities Scholarship Foundation.

<sup>1</sup>L. T. Canham, Appl. Phys. Lett. **57**, 1046 (1990); A. G. Cullis, L. T. Canham, and P. D. Calcott, J. Appl. Phys. **82**, 909 (1997).

<sup>2</sup>V. Lehmann and U. Gösele, Appl. Phys. Lett. **58**, 856 (1991).

- <sup>3</sup>D. J. DiMaria, J. R. Kirtley, E. J. Pakulis, D. W. Dong, T. S. Kuan, F. L. Pesavento, T. N. Theis, and J. A. Cutro, J. Appl. Phys. **56**, 401 (1984).
- <sup>4</sup>S. Furukawa and T. Miyasato, Jpn. J. Appl. Phys., Part 2 **27**, L2207 (1988).
- <sup>5</sup>H. Takagi, H. Ogawa, Y. Yamazaki, A. Ishizaki, and T. Nakagiri, Appl. Phys. Lett. **56**, 2379 (1990).
- <sup>6</sup>H. Morisaki, F. W. Ping, H. Ono, and K. Yazawa, J. Appl. Phys. **70**, 1869 (1991).
- <sup>7</sup>S. Hayashi, T. Nagareda, Y. Kanzawa, and K. Yamamoto, Jpn. J. Appl. Phys., Part 1 **32**, 3840 (1993).
- <sup>8</sup>J. F. Ziegler, in *Ion Implantation Technology*, edited by J. F. Ziegler (North-Holland, Amsterdam, 1992), p. 1.
- <sup>9</sup>P. D. Townsend, P. J. Chandler, and L. Zhang, *Optical Effects of Ion Implantation* (Cambridge University Press, Cambridge, 1994).
- <sup>10</sup>T. S. Iwayama, M. Ohshima, T. Niimi, S. Nakao, K. Saitoh, T. Fujita, and N. Itoh, J. Phys.: Condens. Matter **5**, L375 (1993).
- <sup>11</sup>T. S. Iwayama, K. Fujita, S. Nakao, K. Saitoh, T. Fujita, and N. Itoh, J. Appl. Phys. **75**, 7779 (1994).
- <sup>12</sup>N. Itoh, T. S. Iwayama, and T. Fujita, J. Non-Cryst. Solids **179**, 194 (1994).
- <sup>13</sup>T. S. Iwayama, S. Nakao, and K. Saitoh, Appl. Phys. Lett. **65**, 1814 (1994).
- <sup>14</sup>T. S. Iwayama, S. Nakao, K. Saitoh, and N. Itoh, J. Phys.: Condens. Matter **6**, L601 (1994).
- <sup>15</sup>P. Mutti, G. Ghislotti, S. Bertoni, L. Bonoldi, G. F. Cerofolini, L. Meda, E. Grilli, and M. Gruzzi, Appl. Phys. Lett. **66**, 851 (1995).
- <sup>16</sup>H. A. Atwater, K. V. Shcheglov, S. S. Wong, K. J. Vahala, R. C. Flagan, M. L. Brongersma, and A. Polman, Mater. Res. Soc. Symp. Proc. **316**, 409 (1994); K. S. Min, K. V. Shcheglov, C. M. Yang, H. A. Atwater, M. L. Brongersma, and A. Polman, Appl. Phys. Lett. **69**, 2033 (1996).
- <sup>17</sup>P. Mutti, G. Ghislotti, S. Bertoni, L. Bonoldi, G. F. Cerofolini, L. Meda, E. Grilli, and M. Gruzzi, Appl. Phys. Lett. **66**, 851 (1995).
- <sup>18</sup>J. G. Zhu, C. W. White, J. D. Budai, S. P. Withrow, and Y. Chen, Mater. Res. Soc. Symp. Proc. **358**, 163 (1995); H. M. Cheong, W. Paul, S. P. Withrow, J. G. Zhu, J. D. Budai, C. W. White, and D. M. Hembree, Jr., Appl. Phys. Lett. **68**, 87 (1996).
- <sup>19</sup>T. Komoda, J. P. Kelly, A. Nejm, K. P. Homewood, P. L. F. Hemment, and B. J. Sealy, Mater. Res. Soc. Symp. Proc. **358**, 175 (1995).
- <sup>20</sup>S. Guha, M. D. Pace, D. N. Dunn, and I. L. Singer, Appl. Phys. Lett. **70**, 1207 (1997).
- <sup>21</sup>H. Z. Song, X. M. Bao, N. S. Li, and J. Y. Zhang, J. Appl. Phys. **82**, 4028 (1997).
- <sup>22</sup>J. F. Ziegler, J. P. Biersack, and U. Littmark, *The Stopping and Range of Ions in Solids* (Pergamon, New York, 1985).
- <sup>23</sup>N. Wada and M. Ichikawa, Jpn. J. Appl. Phys. **15**, 755 (1976).
- <sup>24</sup>A. Rosenzweig, *Photoacoustics and Photoacoustic Spectroscopy* (Wiley, New York, 1980), p. 137.
- <sup>25</sup>J. F. McClelland and R. N. Kniseley, Appl. Opt. **15**, 2967 (1976).
- <sup>26</sup>T. Takagahara and K. Takeda, Phys. Rev. B **42**, 9664 (1992).
- <sup>27</sup>Y. Kanemitsu, H. Uto, Y. Masumoto, and Y. Maeda, Appl. Phys. Lett. **61**, 2187 (1992).
- <sup>28</sup>T. Fischer, V. P.-Koch, K. Shcheglov, M. S. Brandt, and F. Koch, Thin Solid Films **275**, 100 (1996).
- <sup>29</sup>W. Skorupa, R. A. Yankov, I. E. Tyschenko, H. Fröb, T. Böhme, and K. Leo, Appl. Phys. Lett. **68**, 2410 (1996).